13th World Conference on Earthquake Engineering
Vancouver, B.C., Canada
August 1-6, 2004
Paper No. 204

EVALUATE OF SOURCE TIME FUNCTION OF ALBORZ REGION AND SURROUNDING AREA EARTHQUAKES

Mehrdad MOSTAFAZADEH [1]

SUMMARY

The Alborz region is a relatively seismic block within the Alpine-Himalayan Belt. We have compiled source time function of 31 events of Caspian earthquakes that is obtained from teleseismic body waveform modeling. The duration of each subevent with magnitude larger than 5 (M_w >5.0) and depth between 4≤ h≤76 km was determined from source time function. When viewed over the entire depth range, the total duration (τ_t) is related to M_o by $\log \tau_t = (0.2642 \pm 0.001) \log M_O$ _8.9119 ($\pm$.0.194).

INTRODUCTION

Earthquake source time duration is an important characteristic of the rupture process. Whereas shallow earthquakes can be explained by a process involving simple failure or slip on a frictional surface, the mode of stress release at depths where the overburden pressure is too large to allow for simple frictional sliding is still a matter of much debate. Because of its dependence upon important characteristics of the rupture such as fault size, stress drop, and rupture velocity, earthquake duration is a potentially powerful, if somewhat imprecise; discriminate between mechanical models of deep earthquakes.
Body waveform modeling has become one of the most important tools available to seismologist for refining earth structure models and understanding fault-rupturing process. Three component waveform data from the far-field GDSN stations in the epicentral range 30^0- 90^0 were obtained for the selected earthquakes. SYN3 algorithm [1] and IASPEI SYN4 algorithm [2], which is a recent version of Nabelek, [3] inversion procedure based on a weighted least squares method, was used for waveform inversion. The source time function (described by a series of overlapping isosceles triangles), centroid depth, and the fault orientation parameters (strike, dip, and the rake) are used in order to compute synthetic seismograms and the seismic moment [4, 5].
In terms of the details of fault rupture or source complexity, our knowledge of the very largest earthquakes is limited. Until recently, most of what was known about major earthquakes consisted of estimates of their focal mechanism and moment. Although this information is of fundamental interest, it is desirable to know more about the spatial and temporal distribution of moment release [6] . The teleseismic source time

[1] International Institute of Earthquake Engineering and Seismology, Iran, e-mail:mehrdad@iiees.ac.ir

function gives information about fault rupture or source complexity. The relationship between seismic moment, M_O, and source duration, τ_t, provides information on regarding the mechanics of faulting in the earth's interior. In this paper we present the results of a survey study of teleseismic source time functions for major shallow earthquakes in south of Caspian Basin and surrounding area studied by Priestley [4] and Jackson [5], Table 1. The disadvantage of forward modeling is that the uniqueness of the solution is not easily assessed. Inverse techniques, on the other hand, have made it practical to observe the trade-off one variable with respect to another [7].

Defining the link between the radiated seismic waves of earthquakes and fault properties is the central problem in eartquake seismology. Brune [8, 9] gave a rather simple set of formulas that allowed the determination of stress drop, source radius, corner frequency and moment from spectra of the body wave. The possibility that there is a relation between the seismic stress drop and shear stress on the fault suggested that a synthesis of stress drop values might yield insight into the level of stress on the fault, spatial and temporal variations in shear stress, and even the stresses that drive the plate motions. There is some suggestion that earthquakes from different tectonic regions have systematically different values of apparent stress or stress drop [10].

The essential purpose of this study is to evaluate fault rupture or source complexity, and prepare information about time history of displacement on the fault. In addition we want to evaluate the seismic moment -duration and interpret any relation between stress drop and depth of earthquakes (Table 1). And finally we want to introduce a rupture model map for of seismic events those are occurred in Caspian and surronding area. Figure 1 shows the disribution of epicenter location of earthquakes that are used in this study.

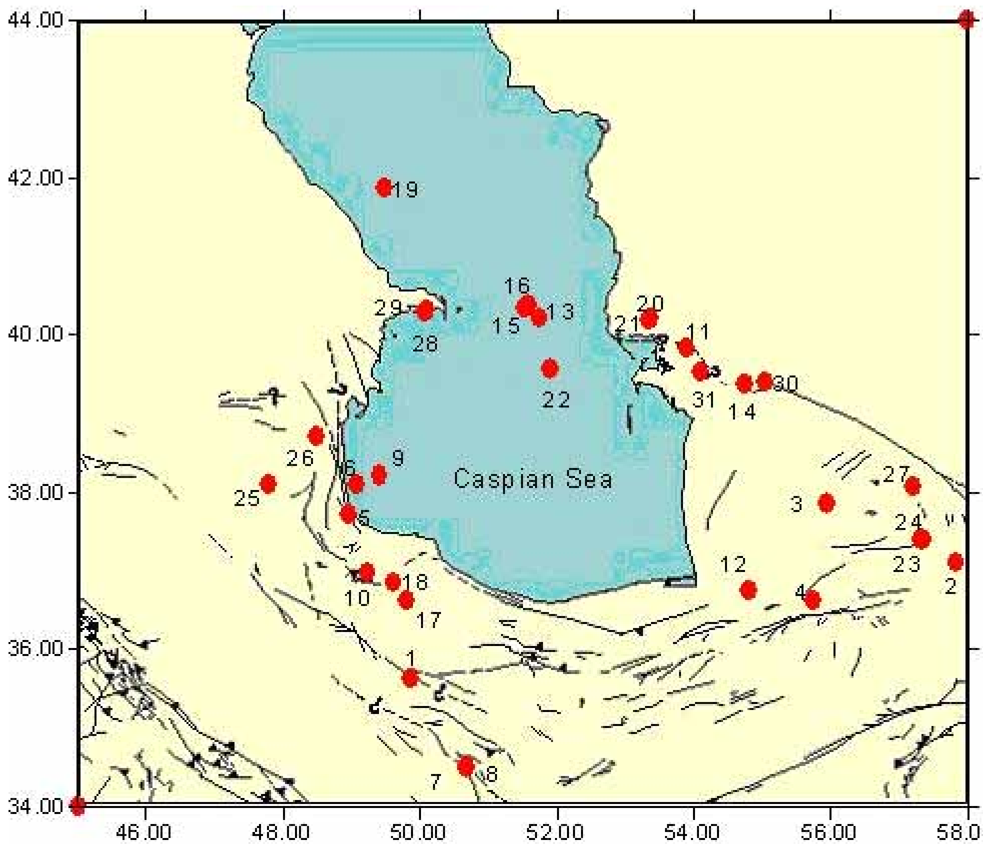

Fig 1: Map showing the distribution of epicenter of earthquakes studied in this paper (Table 1).

Table 1. Earthquake hypocentral data [4, 5].

No	Date d m y	Origin time	Latitude (N^0)	Longitude (E^0)	Depth (Km)	M_w	M_O(N-m)
1	01 09 1962	19:20	35.63	49.87	10	7.0	3.68E+19
2	03 01 1969	03:16	37.10	57.83	7	5.5	1.89E+17
3	30 07 1970	00:52	37.85	55.94	11	6.3	4.29E+18
4	14 02 1971	16:27	36.62	55.74	11	5.7	4.05E+17
5	04 11 1978	15:22	37.71	48.95	21	6.1	1.90E+18
6	04 05 1980	18:35	38.09	49.07	15	6.3	4.02E+18
7	19 12 1980	01:16	34:50	50.67	14	6.0	1.40E+18
8	22 12 1980	12:51	34.49	50.67	15	5.6	2.81E+17
9	04 08 1981	18:35	38.21	49.41	20	5.6	2.38E+17
10	22 07 1983	02:41	36.98	49.23	10	5.6	1.88E+17
11	22 02 1984	05:44	39.52	54.11	27	5.7	5.10E+17
12	29 10 1985	13:13	36.75	54.81	13	6.2	2.18E+18
13	06 03 1986	00:05	40.37	51.60	35	6.2	2.43E+18
14	07 09 1987	11:32	39.37	54.76	30	5.5	2.33E+17
15	16 09 1989	02:05	40.34	51.53	31	6.5	6.84E+18
16	17 09 1989	00:53	40.20	51.75	35	6.2	2.17E+18
17	21 06 1990	09:02	36.61	49.81	10	5.6	2.91E+17
18	28 11 1991	17:20	36.84	49.61	8	5.7	3.89E+17
19	31 08 1993	06:55	41.87	49.47	76	5.1	6.33E+16
20	01 07 1994	10:12	40.19	53.35	42	5.6	2.93E+17
21	01 07 1994	19:50	40.20	53.37	41	5.1	5.95E+16
22	29 10 1995	06:27	39.56	51.90	61	5.3	1.22E+17
23	04 02 1997	09:53	37.39	57.33	13	5.4	1.61E+17
24	04 02 1997	10:37	37.39	57.35	8	6.4	5.75E+18
25	28 02 1997	12:57	38.10	47.79	9	6.0	1.20E+18
26	09 07 1998	14:19	38.71	48.50	27	5.6	4.38E+17
27	22 08 2000	16:55	38.07	57.19	4	5.6	3.09E+17
28	25 11 2001	18:09	40.29	50.06	40	6.2	2.34E+18
29	25 11 2000	18:10	40.31	50.09	33	6.1	1.67E+18
30	06 12 2000	17:11	39.40	55.04	31	6.9	2.41E+19
31	10 06 2001	01:52	39.83	53.89	31	5.3	1.17E+17

Previous Works

Three measures of source duration of an earthquake have been reported in the literature (Fig.2 taken from Singh ,[11]: the total rupture duration (τ_t), the pulse duration of each subevent of a complex earthquake (τ_p), and rise time (τ_r) [11].

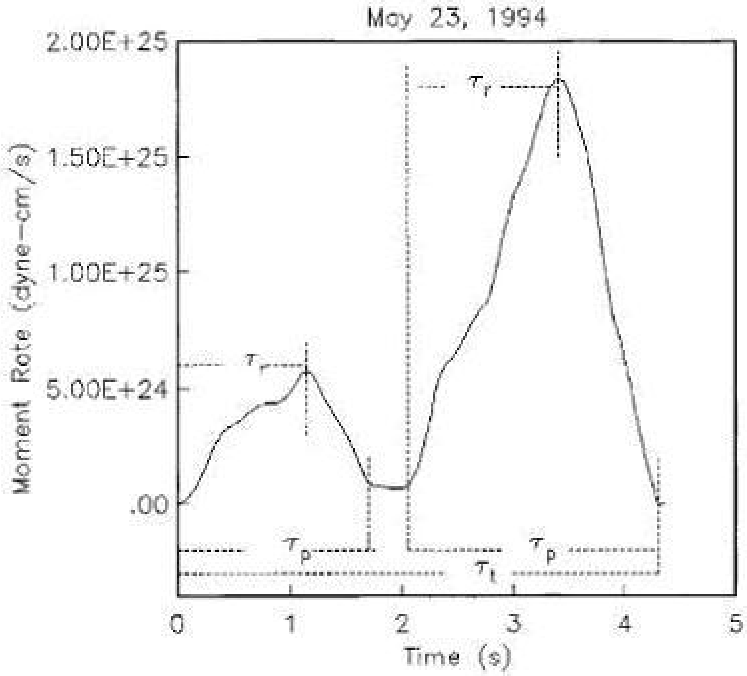

Fig 2: An example of three measures of source duration of an earthquake [11].

It is well known that a constant stress drop source model implies that M_o/τ^3 is a constant. For shallow earthquakes the reported values of M_o/τ_t^3 lie between 0.25×10^{23} and 1.0×10^{23} dyne cm/s^3 [12, 13, 14, 15]. These results were obtained from the analysis of teleseismic data. Kikuchi and Ishida [16] studied source time function (STF) and subevent pulse duration, τ_p, of earthquakes in the Kanto region of Japan, which were recorded by broadband seismographic network near the epicentral region. Focal depths of Kanto earthquakes were examined had focal depths between 50 and 125 km [16]. Kikuchi and Ishida [16] reported to be of $M_O/\tau^3_p \sim 1\times10^{24}$ dyne cm/s^3 for intermediate seismicity. Bos [17] studied about source duration and depth of deep (h > 300 km) earthquakes, and they have observed a slight decrease in duration with depth. They have suggested total durations satisfy a least square fit of

$t_{tot} = (9.77 \pm 0.28) - (3.59 \pm 0.82) \times 10^{-3}$ H

where earthquake depth H is in kilometers and t is in seconds.

Fault Complexity and Age of Lithosphere

The source complexity of the earthquakes is appraised by the physical features of the teleseismic source time functions. These features include the overall duration, multiple or single event character. Individual source pulse widths, and roughness of the time function. The above measures of source size and complexity can then be compared with the age of subducted lithosphere, plate convergence rate, and other physical parameters of subduction zone [6]. Such comparisons are important for increasing our understanding of the worldwide distribution of the largest earthquakes and their radiated energy. Recent studies of large subduction zone earthquakes suggest that the maximum observed earthquake for a given trench is directly related to the degree of coupling between the plates and the size of fault asperities [18]. Ruff and Kanamori [19] found a significant relationship between the age of the subducting lithosphere, convergence rate, and maximum M_w. Trenches subducting younger crust with higher convergence rates were found in general to produce larger earthquakes. Higher convergence rates and younger, more buoyant crust are thought to cause larger earthquakes by producing strong coupling between the plates. In the asperity model of subduction zone earthquakes, stronger coupling is a direct result of greater areas of the fault plane supporting the accumulated stress between the plates. These areas rupture relatively coherently during and earthquake and are termed asperities.

The earthquakes larger than about M_s 6.9 can rarely be represented by a single point source, even at the wavelengths recorded by the WWSSN 15-100 long period instruments (with a peak response at about 15s period). These earthquakes usually consist of several discrete ruptures, separated by several seconds in time and several km in space, often occurring on faults with different orientations [20]. This is believed to be an expression of fault complexity the heterogeneity of the faulting process at the earthquake source. Two models have been proposed to explain this heterogeneity; the barrier model [21] and the asperity model [22].

INTERPRETATION AND DISSCUSION

SEPTEMBER 1, 1962 EARTHQUAKE (NO; 1)

Source time function (STF) shows different time characteristics of energy release (Figure 3). The 1962 September 1 Buyin Zahra earthquake (M_S 7.2, m_b 6.9) devastated the area south of Qazvin in northern Iran, killing around 12200 people [23]. A displacement generally implies an oblique faulting involved both thrusting on planes dipping south and also left-lateral strike-slip. Average amplitudes were about 1.4m vertical displacement and 0.6m strike slip [4]. The natures of source time function complexity of two-subevent show that the most part of seismic moment release in rise (stress increase) and fall (stress decrease) time portion. However we can see the source time function has near 7-second flat duration between two subevent that is relation to lowest stress accumulation occurred in this segment. The rise time of the subevent 1 (τ_r ~ 4.6) is greater than subevent 2 (τ_r ~2.5) and pulse duration of both subevent is near to equal. The slow rise time presumably results from a very low stress drop. The small slip (40^0) of this event indicates that asperities are not apparently region of high strength. Because the concentration of slip on asperities implies they are regions of high

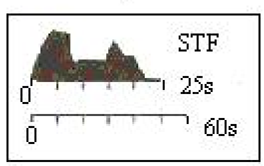

Fig 3: Far-field source time functions of the 1962 Buyin Zahra earthquake showing emergent seismic moment release [4].

moment release, which, in turn, implies a fundamental difference in the fault behavior at the asperity compared with that of the surrounding this fault.

JANUARY 3, 1969 (NO; 2), JULY 30, 1970 (NO; 3), FEBRUARY 22, 1984 (NO; 11), MARCH 6, 1986 (NO; 13), FEBRUARY 14, 1971 (NO; 4), SEPTEMBER 17, 1989 (NO; 16), NOVEMBER 28, 1991 (NO;18), EARTHQUAKES.

These earthquakes have larger moment release in the first part of the process, while ratios of subevents for foreshock of events number 13, 18 occurs in the last part and initiate with small release followed after 4s and 2s by a larger one respectively (Figure 4). Events 3, 11, 16 show a complex rupture process formed more than 2 subevents. In conjunction with the spatial and temporal behavior of these events the complexity of rupture suggests that strain accumulated gradually on a system of faults in the sediments, granitic and basaltic region [4]. The effect of a critical rupture (the first event of the main shock) was to cause a rapid release of stress (dominant event of the main shock) as well as a more gradual release of stress (the other subevents) on adjacent coplanar and conjugate faults.

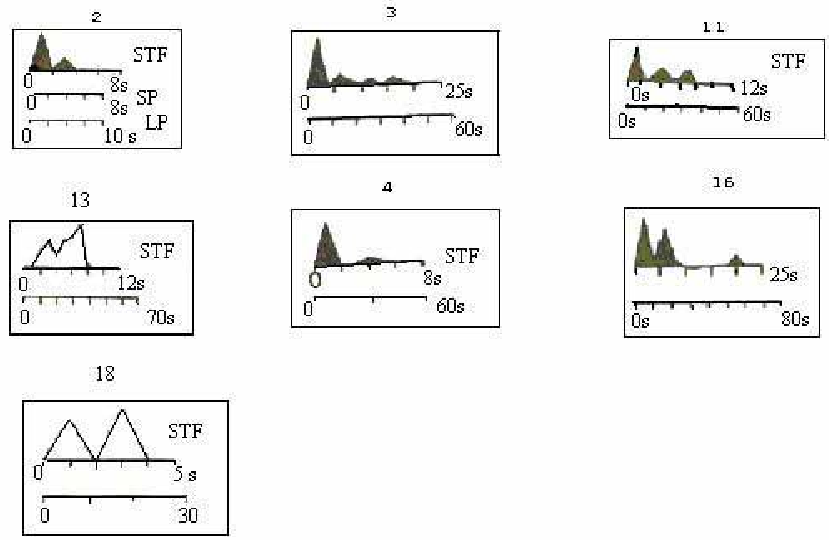

Fig 4: Far-field source time functions of the 3 January 1969, 30 July 1970, 22 February 1984, 6 March 1986, 14 February 1971, 17 September 1989, 28 November 1991 earthquakes showing emergent seismic moment release [4, 5].

NOVEMBER 4, 1978 (NO; 5), DECEMBER 19, 1980 (NO; 7),SEPTEMBER 7, 1987 (NO; 14) , SEPTEMBER 16, 1989(NO; 15), MAY 4, 1980 (NO; 6), AUGUST 31, 1993 (NO; 19), JULY 1. 1994 (NO; 20), OCTOBER 29, 1995 (NO; 22), FEBRUARY 4, 1997 (NO;24), FEBRUARY 28, 1997 (NO; 25), 09 JULY 1998 (NO; 26), 22 AUGUST 2000 (NO; 27), 25 NOVEMBER 2000 (NO;28), DECEMBER 6, 2000 (NO;30) EARTHQUAKES

Figure 5 displays the source time functions of these earthquakes. All STF (except event 24) start with a high release of energy in first part of subevent one. Varying the seismic moment along total duration of STF is direct related to varying the source velocity structure did have an effect on centroid depth and seismic moment. In addition uncertainties in attenuation factor, t^*, mainly affect estimates of source duration and seismic moment. The STF of these events show that the rupture characteristics contain a different size of subevents with same shape and same rupture history. The rise time of subevent 1 is larger than another subevents and most part of seismic moment release in first rupturing process. The nature of this function show that the faulting consists of several fractures separated by strong barriers, which remain unbroken after the event. If the barriers are completely broken, there may be no aftershocks within the main-shock fault plane. The emergent nature of the seismic moment release observed in the rise time of the source time function suggests the no difficulties in breaking the barriers. Earthquake with larger magnitude ($M_w \geq 6$) show long duration and complex STF (events 15, 24, 25, 28, 30). Events 15 and 24 show a complex rupture process formed by a 3 subevents, with a shorter STF for the first one and near to equal duration for event 28. The complexity of the source time function as evidenced by the complexity of the body phases, low fault rupture velocity, is explained in terms of a multiple source.

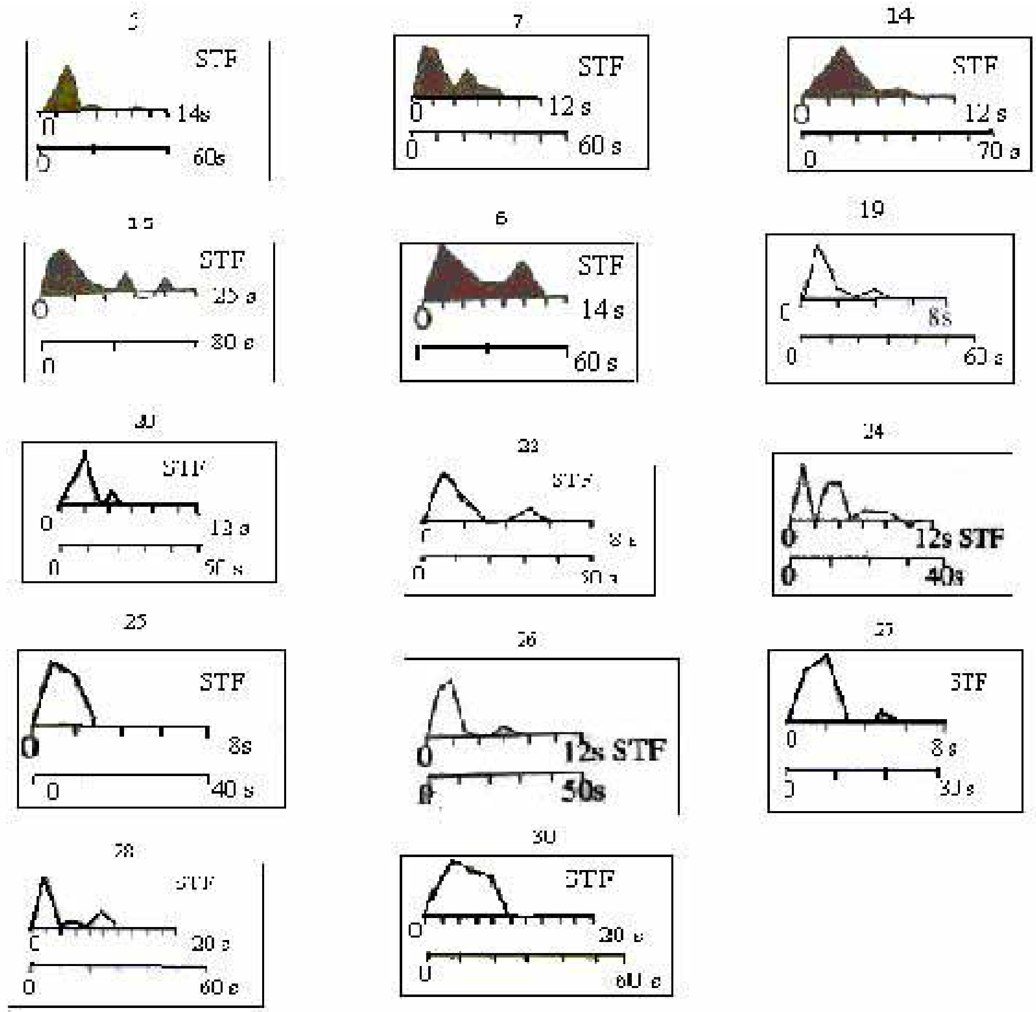

Figure 5: Far-field source time functions of the 4 November 1978, 19 December 1980, 7 September 1987, 16 September 1989, 4 May 1980, 31 August 1993, 01 July 1994, 29 October 1995, 04 February 1997, 28 February 1997, 09 July 1998, 22 August 2000, 25 November 2000, 06 December 2000 earthquakes showing emergent seismic moment release [4, 5].

OCTOBER 29, 1985 (NO; 12), DECEMBER 22, 1980 (NO; 8), AUGUST 4, 1981 (NO; 9), JULY 22, 1983 (NO; 10), JUNE 21, 1990 (NO; 17), JULY 1, 1994 (NO; 21), FEBRUARY 4, 1997 (NO; 23), NOVEMBER 25, 2000 (NO; 29), JUNE 10, 2001 (NO; 31) EARTHQUAKES

Figure 6 displays the source time function of these events. Earthquakes 12, 8, 9, 23 have larger moment release in the first part of the process and consist several impulses that can be interpreted as a more complex rupture process. Shallow earthquakes 10, 17, 21, 29, 31 with M_w <6 and epicenter inside the continent show simple STF, in general corresponding to a simple impulse of triangular form with short time duration, less than 5s. These shocks can be associated with single rupture.

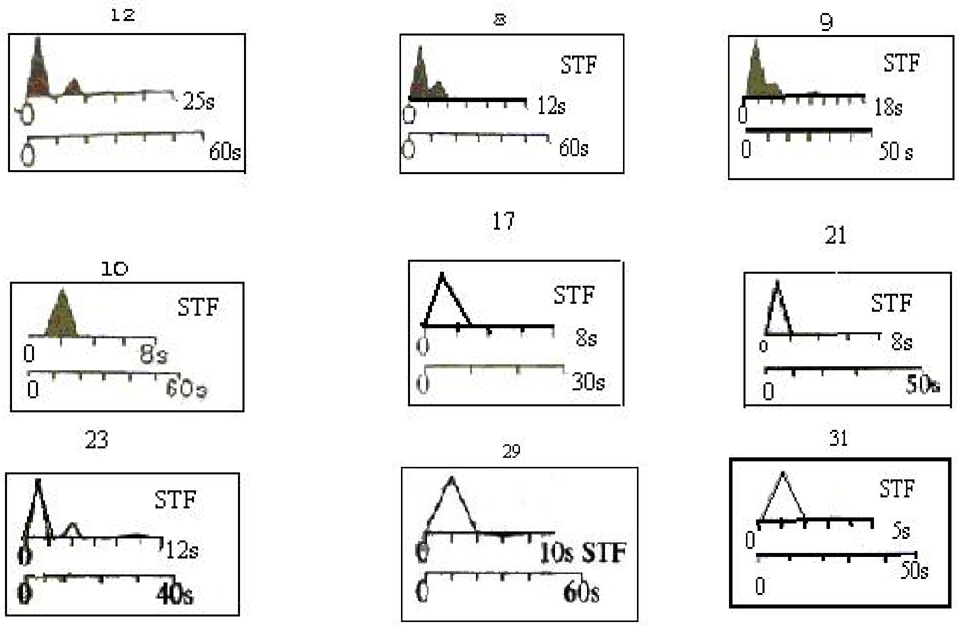

Fig 6: Far-field source time functions of the 29 October 1985, 22 December 1980, 4 August 1981, 22 July 1983, 21 June 1990, 01 July 1994, 04 February 1997, 25 November 2000 earthquakes showing emergent seismic moment release [4, 5].

Source Duration versus Seismic Moment and Depth

Figure 7 shows the measured durations plotted the corresponding moment of total duration. The entire data set is fit by $\log \tau_t = 0.2642 \log M_O$ _8.9119. We have expected that to obtain value lie between $\log \tau \propto 0.25 \log M_o$ and $\log \tau \propto 1.0 \log M_o$ for shallow earthquakes [12, 13, 14, 15]. At expected, events with large moments tend to have longer durations than events with smaller moments. Table 2 show that result of regression, $\log \tau_t = c \log M_o + d$ for different tectonic regions.

Table 2: Result of regression for different tectonic regions.

Region	Total duration	Reference
Caspian sea and surronding area	C = 0.264 ± 0.0001 d = -8.911± 0.194	This study
Mexico	C = 0.363 ± 0.014 d = -8.619 ± 0.337	Singh et. al., 2000
Mexico and Kanto	C = 0.365 ± 0.011 d =- 8.706 ± 0.262	Singh et. al., 2000
Mexico, Kanto, California, and deep	C = 0.363 ± 0.008 d = -8.580 ± 0.190	Singh et. al., 2000

Comparison of C parameter between above different tectonic region shows that the Caspian sea and surronding area has lowest slop than other region. The seismicity in Caspian sea and surronding area has continental intraplate characteristics. But the seismic activities in Mexico, Kanto and California regions have oceanic interplate features. The comparison of homogeneity between both different tectonic regions shows that this parameter in oceanic plate is more than continental plates. In addition the seismic signal in this area (oceanic interplate) is less attenuate than other continental itraplate region. In this reason the body wave phases with longer duration can be observed in oceanic interplate regions than continental intraplate area. We can see clearly the slop value in oceanic plate is greater than Caspian and surronding area.

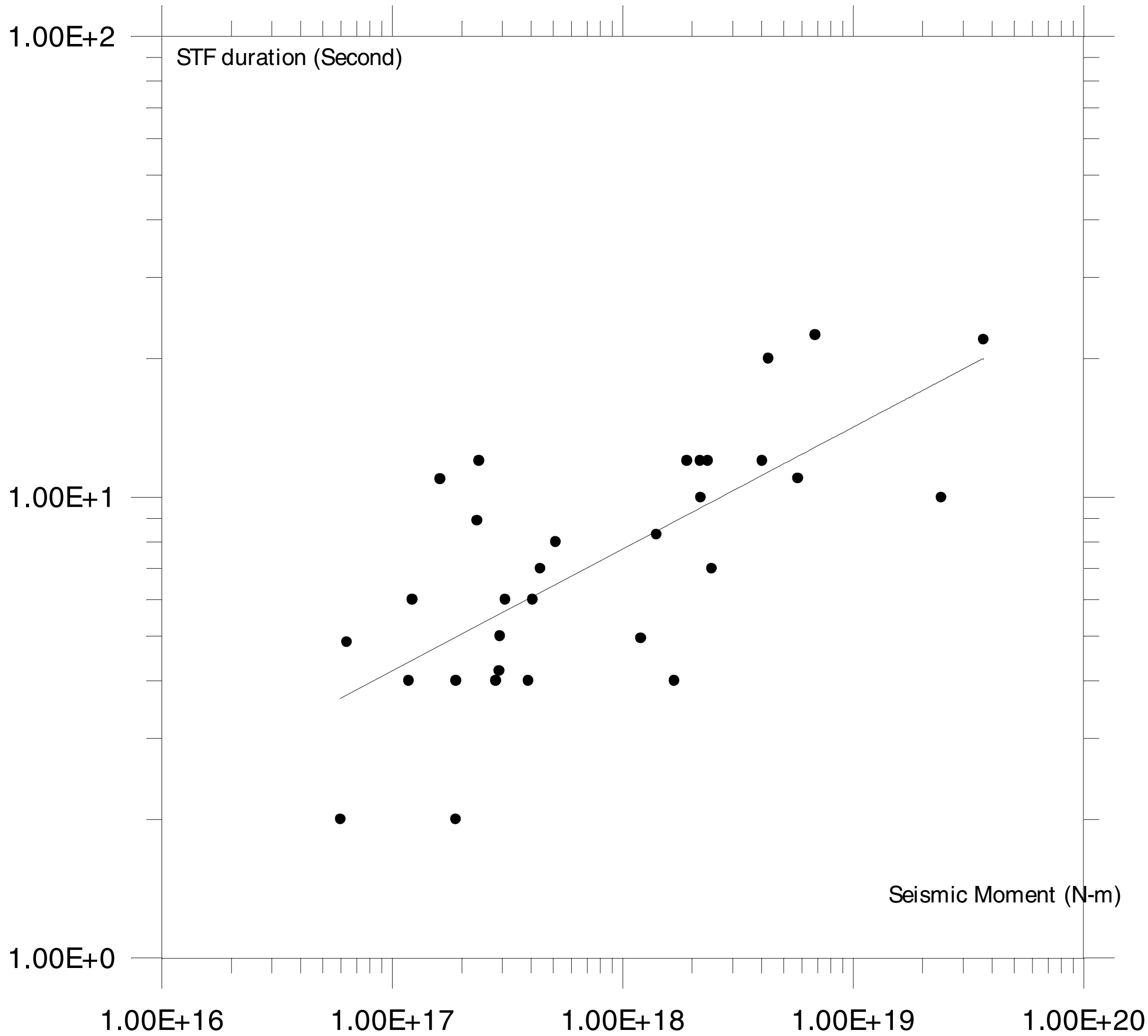

Fig 7: Source duration (τ_t) versus seismic moment (M_O).

CONCLUSIONS

In this study we search for source characteristics detectable from source time function to examine if there is any depth dependence in source properties for crustal earthquakes. We do not find any clear depth dependence with source duration. The source time function of these earthquakes show that the faulting in the Caspian region consists of several fractures separated by strong barriers, which remain unbroken after the event. If the barriers are completely broken, there may be no aftershocks within the main-shock fault plane. Source time functions show different characteristics depending on the magnitude and depth of the earthquakes. Shallow earthquakes located offshore with large magnitude show complex STF and long time duration. Within the continent shallow earthquakes show less complexity and STF have shorter duration.

REFERENCES

1. McCaffery, R. & Abers. G. Syn3 : A program for inversion of Teleseismic Body Wave Forms on Microcomputers, Air Force Geophysics Laboratory Technical Reoprt, AFGL-TR-88-0099. Hanscomb Air Force Base, MA 1988.

2. McCaffery, R. Abers, G. & Zwick P,. Inversion of teleseismic body waves. In: Digital seismogram analysis and waveform inversion (ed. By W. H. K. Lee), IASPEI software Library, 1991; 3,81-166.

3. Nabelek, J. L., . Determination of earthquake source parameters from inversion of body waves, PhD thesis, MIT, Cambridge, MA 1984.

4. Priestly, K. Baker, C., Jackson, J . Implication of earthquake focal mechanism data for the active tectonics of the south Caspian basin and surrounding regions, Geophys. J. Int., 1994; 118, 111-141.

5. Jackson, J. Priestly, K. Allen, M. Berberian, M. Active tectonics of the South Caspian Basin, Geophys. J. Int. 2002: 148, 214-245.

6. Hartzell, S. and T.Heaton . Teleseismic time functions for large, shallow subduction zone earthquakes, Bull. Seism. Soc. Am. 1985; 75 (4): 965-1004.

7. Christensen, Douglas H. and Ruff, Larry J., . Analysis of the trade- off between hypocentral depth and source time function, Bull. Seism. Soc. Am. 1985; 75 (6): 1637-1656.

8. Brune, J. N., . Tectonic stress and the spectra of seismic shear waves from earthquakes, J. Geophys. Res., 1970; 75: 4997-5009.

9. Brune, J. N., . Tectonic stress and the spectra of seismic shear waves from earthquakes: correction, J. Geophys. Res, 1971; 76: 5002.

10. Wyss, M. and J. N. Brune,. Regional variations of source properties in southern California estimated from the ratio of short to long period amplitudes, Bull. Seism. Soc. Am. 1971; 61: 1153-1168.

11. Singh, k. Pacheco, J. Ordaz, M. and V, Kostoglodov. Source time function and duration of Mexican earthquakes, Bull. Seism. Soc. Am. 2000; 90 (2): 468-482.

12. Kanamori, H., and J.W.Giwen . Use of long period surface waves for rapid estimation of earthquake source parameters, Phys. Earth Planet, Interiors 1981; 27: 8-31.

13. Furumoto, M., and I. Nakanishi . Source time scaling relation of large earthquakes, J. Geophys. Res. 1983 ; 88: 2191-2198.

14. Ekstom , G., R.Engahl . Earthquake source parameters and stress distribution in the Adak Island region of the central Aleutians Islands, J. Geophys. Res. 1989; 94: 15499-15519.

15. Ekstom, G., R. S. Stein, J. P. Eaton, and D. Eberhart-Phillips . Seismicity and geometry of a 100-km long blind thrust 1. The 1985 Ketleman Hills, California earthquake, J. Geophys. Res. 1992; 97: 4843-4863.

16. Kikuchi, M., and M. Ishida . Source retrieval for deep local earthquakes with broadband records, Bull. Seism. Am. 1993: 83: 1855-1870.

17. Bos , A. G., G. Nolet., A. Rubin., H. Houston., and J. E. Vidale., . Duration of deep earthquakes determined by stacking of Global seismograph Network seismograms, J. Geophys. Res., 1998; 103 (B9): 21,059-21,065.

18. Uyeda. S. and H. Kanamori . Bac- arc opening and the mode of the sub-ducting, J. Geophys., Res., 1983; 84: 1049-1061.

19. Ruff, L. and H. Kanamori . Seismicity and the subduction process, Phys. Earth Planet. Interiors 1980; 23, 240-252.

20. Butler, R., Stewart, G. S. and Kanamori, H., . The July 27 1976 Tangshan China earthquake –a complex sequence of intraplate events, Bull. Seism. Soc. Am., 1979; 69: 207-220.

21. Das, S. & Aki, K., . Fault plane with barriers: a versatile earthquake model, J. Geophys. Res., 1977; 82: 5658-5670.

22. Kanamori, H. & Stewart, G. S., . Seismological aspects of the Guatemala earthquake, J. Geophys. Res., 1978; 83: 3427-3434.

23. Ambraseys, N. N., . The Buyin Zahra (Iran) earthquake of September 1962: a field report, Bull. Soc. Am., 1963; 53: 705-740.